Hindawi Publishing Corporation
Mathematical Problems in Engineering
Volume 2012, Article ID 472575, 16 pages
doi:10.1155/2012/472575

Research Article

A Determination of an Abrupt Motion of the Sea Bottom by Using Snapshot Data of Water Waves

T. S. Jang,[1] Hong Gun Sung,[2] and Jinsoo Park[1]

[1] *Department of Naval Architecture and Ocean Engineering, Pusan National University, Busan 609-735, Republic of Korea*
[2] *Maritime and Ocean Engineering Research Institute, Daejeon 305-343, Republic of Korea*

Correspondence should be addressed to T. S. Jang, taek@pusan.ac.kr

Received 20 June 2011; Revised 17 September 2011; Accepted 8 October 2011

Academic Editor: Mohammad Younis

This paper presents an inverse problem and its solution procedure, which are aimed at identifying a sudden underwater movement of the sea bottom. The identification is mathematically shown to work with a known snapshot data of generated water wave configurations. It is also proved that the problem has a unique solution. However, the inverse problem is involved in an integral equation of the first kind, resulting in an ill-posed problem in the sense of stability. That is, the problem lacks solution stability properties. To overcome the difficulty of solution instability, in this paper, a stabilization technique, called regularization, is incorporated in the present solution procedure for the identification of the sea bottom movement. A numerical experiment is presented to demonstrate that the proposed (numerical) solution procedure operates.

1. Introduction

In the field of natural science and ocean engineering, it is not only of interest but important to examine how waves are generated in the ocean surface by the underwater abrupt movement of the sea bottom. If we knew the information of the underwater abrupt movement in advance, it would enable us to determine how the waves propagate in space and time. In practice, this can be extremely crucial, for example, for a Tsunami Warning System (TWS), which is used to detect tsunamis and issue warnings to prevent loss of life and property.

The problem of finding the resulting wave flow field has been usually solved based on the potential wave model. For example, excellent research has been made on the subject of wave generation and propagation [1–4]. Even if much progress has been achieved in determining the resulting wave flow (or forward problem), only few attempts have been

made so far on analysis of an inverse problem to the resulting wave flow. The present study concentrates on the cause of the resulting wave flow (or inverse problem).

Recently, Jang et al. [5] have considered a problem that involves the indirect measurement of the movement of the sea bottom when the time history of the resulting wave motion is observed. They proposed a procedure for finding the wave source based on time-history data acquisition. Although the procedure by Jang et al. [5] is robust for measuring the wave source, it requires a relatively long time to acquire the time-history data at a fixed measurement position. However, in some cases, it may be convenient to obtain a snapshot data of the resulting wave configuration, for example, using a high-speed Remote Control airplane camera, rather than the acquiring of the full-time history data.

Motivated by this, we propose, in this paper, a new systematic procedure for the indirect measurement of abrupt underwater movement of the sea bottom by analyzing "snapshot" data of a local wave configuration. That is to say, the only needed data for identifying the underwater wave source is a snapshot involving a local wave configuration such as wave photos [2] taken from a remote control airplane at a fixed time. It is interesting to note that the new procedure proposed is also suitable to recover whole (or global) wave configurations only by using a local data of wave configuration. This work is classified as an inverse problem which occurs in many branches of science and engineering [5–15].

As a first step, we begin with a simplified mathematical wave model. That is, the two-dimensional irrotational wave flow is modeled with a constant water depth within the framework of linear dispersive wave theory. Based on the wave model, we propose an inverse problem characterized by an integral equation. The problem proposed is shown to have a unique solution of wave source. However, the problem lacks solution stability properties. This means that a small amount of noise from the snapshot data may be amplified, eventually leading to unreliable solutions due to the lack of stability. This is an unwelcome instability phenomenon which contrasts to the usual well-posed problem arising in natural sciences. A stabilization technique is applied to overcome this difficulty [16].

We investigate the workability of our approach through a numerical experiment. Although this work is a fundamental first step toward the indirect measurement of underwater movement, it may be related to a problem concerning the nature of tsunami generation using photographic (or snapshot) wave configuration. This, in turn, provides the basis for a photographic identifying problem for wave sources such as submarine-landslide, earthquakes, and underwater explosions or the testing of nuclear weapons [17–21].

2. Transient Waves by Abrupt Movement of Sea Bottom

We consider an inviscid incompressible water of finite depth and a system of coordinates in which the y-axis is vertical and the x-axis horizontal in mutually perpendicular directions, as shown in Figure 1. The water is assumed to have a constant density and negligible surface tension. The surface water waves are induced in the body of the water (initially at rest for time $t < 0$) by an abrupt movement of the sea bottom.

2.1. Boundary Conditions

We assume that the flow is irrotational in a simply connected fluid domain such that there exists a single-valued velocity potential function $\Phi(x, y, t)$. Then, by the continuity equation, in the system of Cartesian coordinates (x, y), the free-surface wave motion is governed by the

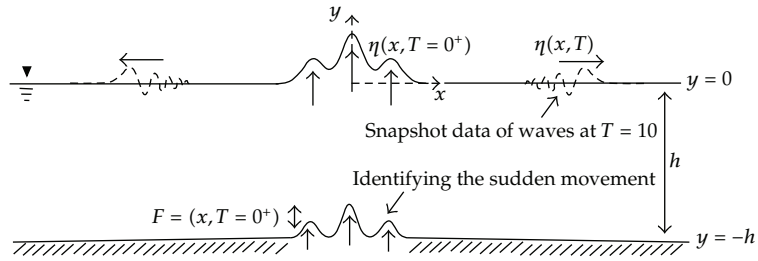

Figure 1: Impulsive movement of the sea-bottom and the resulting wave flow.

elliptic type of Laplace equation with regard to the velocity potential $\Phi(x, y, t)$

$$\frac{\partial^2 \Phi}{\partial x^2} + \frac{\partial^2 \Phi}{\partial y^2} = 0, \tag{2.1}$$

because water is assumed to be incompressible. The kinematic and dynamic free-surface boundary conditions are imposed on the mean free surface, $y = 0$, respectively as

$$\begin{aligned} \frac{\partial \eta}{\partial t} &= \frac{\partial \Phi}{\partial y}, \\ \frac{\partial \Phi}{\partial t} + g\eta &= 0, \end{aligned} \tag{2.2}$$

where $\eta(x, t)$ denotes the free-surface elevation, and g is the gravity acceleration [1]. Denoting the sea bottom displacement by

$$y = -h + F(x, t), \tag{2.3}$$

the boundary condition of the sea bottom is written as [1]

$$\frac{\partial \Phi}{\partial y} = \frac{\partial F}{\partial t} \quad \text{on } y = -h. \tag{2.4}$$

2.2. *Wave Spectrum*

We suppose that the sea bottom changes suddenly at $t = 0$ such that its movement can be mathematically expressed as

$$F(x, 0^-) = 0, \qquad F(x, 0^+) = F_0(x). \tag{2.5}$$

Applying Fourier-Laplace transform to the velocity potential in the governing equation (2.1) and the boundary conditions of (2.2) and (2.4), we can derive the wave elevation of the free-surface [1]

$$\eta(x,t) = \int_{-\infty}^{\infty} A(k)\left\{e^{i(kx+\omega t)} + e^{i(kx-\omega t)}\right\}dk \tag{2.6}$$

by using the method of inverse Fourier-Laplace transforms. The resulting wave system of (2.6) is of dispersive waves, whose dispersion relation (between the wave-number k and the frequency ω) and the spectrum $A(k)$ are

$$\omega(k) = \sqrt{gk\tanh kh}, \qquad A(k) = \frac{1}{4\pi}\cdot\frac{\widetilde{F}_0(k)}{\cosh kh}, \tag{2.7}$$

respectively [1–3]. Here, the notation $\widetilde{F}_0(k)$ stands for the Fourier transform $\mathbb{F}$ of $F_0(x)$ and is expressed as follows:

$$\widetilde{F}_0(k) = \mathbb{F}\{F_0(x)\} = \int_{-\infty}^{\infty} e^{-ikx}F_0(x)dx. \tag{2.8}$$

3. Integral Equation

As mentioned before, the abrupt bottom motion is assumed to arise at $t = 0$. The resulting wave system propagates in space with time, according to the dispersion relation equation (2.7). In this study, we will measure the spatial wave distribution of the resulting wave at an instant of time $t = T > 0$, which is symbolized as (3.1)

$$\eta_T = \eta(x,T), \quad -\ell < x < l \tag{3.1}$$

for some real positive constant $\ell > v_g \cdot T : v_g$ is the group velocity, $v_g = (gh)^{1/2}$ [1]. We then are able to find a relationship between the spectrum $\widetilde{F}_0(k)$ in (2.8) and the η_T from (2.6) and (2.7)

$$\eta_T = \eta(x,T) = \int_{-\infty}^{\infty} K(x,T,k)\widetilde{F}_0(k)dk, \quad -\ell < x < l. \tag{3.2}$$

Equation (3.2) can be regarded as an integral equation of the first kind, in which the kernel function K is expressed as

$$K(x,T,k) = e^{ikx}\frac{\cos\left(T\sqrt{gk\tanh kh}\right)}{2\pi\cosh kh}. \tag{3.3}$$

The integral equation (3.2) is rewritten with a symbolic notation as

$$\eta_T = \mathfrak{L}\left(\widetilde{F}_0\right). \tag{3.4}$$

The meaning of the integral equation (3.2) is as follows. If we can measure snapshot data of the surface-wave elevation η_T at $t = T > 0$, it then enables us to identify the spectrum $\widetilde{F}_0(k)$ in (2.6). Physically, this implies that we are able to know completely the whole information of the dispersive wave system in (2.7) if we know a partial information about the wave system, for example, the snapshot data of the surface-wave elevation η_T. We finally discover the abrupt displacement $F_0(x)$ in (2.5) by employing the inverse Fourier transform $\mathbb{F}^{-1}$

$$F_0(x) = \mathbb{F}^{-1}\left\{\widetilde{F}_0(k)\right\} = \frac{1}{2\pi}\int_{-\infty}^{\infty} e^{ikx}\widetilde{F}_0(k)dk. \tag{3.5}$$

4. Uniqueness

Before the detailed discussion of solving the integral equation of (3.2), we need to examine whether the integral equation has a unique solution.

Physically, this is crucial and essential to recover the real movement of the sea bottom. We note that it suffices to prove that the null space of (3.2) is trivial because (3.2) is linear; that is, we want to show that $\eta_T(x) \equiv 0$ identically for $-\ell < x < \ell$ means $\widetilde{F}_0(k) \equiv 0$ identically.

We first rewrite (3.2) as

$$\begin{aligned}\eta_T(x) &= \int_{-\infty}^{\infty} e^{ikx}\frac{\cos\left(T\sqrt{gk\tanh kh}\right)}{2\pi\cosh kh}\widetilde{F}_0(k)dk \\ &= \frac{1}{2\pi}\int_{-\infty}^{\infty}\Phi(k)e^{ikx}dk,\end{aligned} \tag{4.1}$$

where

$$\Phi(k) \equiv \frac{\cos\left(T\sqrt{gk\tanh kh}\right)}{\cosh kh}\widetilde{F}_0(k). \tag{4.2}$$

Thus, the following holds for $-\infty < x < \infty$

$$\eta_T(x) = \mathbb{F}^{-1}\{\Phi(k)\}. \tag{4.3}$$

Alternatively,

$$\Phi(k) = \mathbb{F}\{\eta_T(x)\}. \tag{4.4}$$

From the injectivity of the Fourier transform, we have from (4.3) or (4.4) that the quantity $\Phi(k) \equiv 0$ if $\eta_T(x) \equiv 0$ for $-\infty < x < \infty$. Because the function $\cos(T\sqrt{gk\tanh(kh)})/\cosh(kh)$ in (4.2) has isolated zeros, it follows that $\widetilde{F}_0(k)$ is zero almost everywhere from (4.2). That is, we show that $\eta_T(x) \equiv 0$ identically for $-\infty < x < \infty$ means $\widetilde{F}_0(k) \equiv 0$. Therefore, if $\eta_T(x) \equiv 0$ identically for $-\ell < x < \ell$, $\widetilde{F}_0(k) \equiv 0$. This completes the proof.

5. Construction of the Wave Spectrum

Although the uniqueness of the solution of the wave spectrum has been established, we have still a question of its stability, that is, the solution $\widetilde{F}_0(k)$ depends continuously on the snapshot data of the wave configuration η_T in (3.2).

5.1. The Discontinuous Operator $\mathfrak{L}_c$

Because the computer memory is limited in practice, in this study, we replace the integration limit of ∞ in (3.3) with a large but finite real number κ [5] as follows:

$$\eta_T = \int_{-\kappa}^{\kappa} K(x,T,k)\widetilde{F}_0(k)dk, \tag{5.1}$$

or, in operator notation,

$$\eta_T = \mathfrak{L}_c\left(\widetilde{F}_0\right). \tag{5.2}$$

Equation (5.1) is classified as an integral equation of the first kind rather than the second kind. It is thus necessary to check the stability of the solution, that is, whether it depends on the snapshot wave data in a continuous manner. According to the theory of integral equations, the solution lacks stability properties [5, 16], as the kernel K in (5.1) is regular. This means that a small amount of noisy data in a snapshot wave configuration may be amplified and cause an unreliable solution. In other words, mathematically, the operator $\mathfrak{L}_c$ in (5.2) is discontinuous with respect the usual topology.

5.2. Tikhonov's Regularization

To overcome the difficulty encountered in Section 5.1, we suppress the lack of stability through a stabilization technique. To this end, we suggest the use of the following regularization:

$$q_\alpha = (\alpha I + \mathfrak{L}_c^* \mathfrak{L}_c)^{-1} \mathfrak{L}^* \eta_T \tag{5.3}$$

for a real positive constant α, known as the regularization parameter, where the symbol I is the identity operator and $\mathfrak{L}_c^*$ the adjoint operator of $\mathfrak{L}$ [16, 22–29],

$$(\mathfrak{L}_c^* g)(k) = \int_{-\ell}^{\ell} K(x, T, k) g(x) dx \tag{5.4}$$

for a square integrable function $g(x)$. According to the regularization theory, it is proven that the inverse operator $(\alpha I + \mathfrak{L}_c^* \mathfrak{L}_c)^{-1}$ in (5.3) is bounded and always exists. Moreover, the q_α converges to the solution to (5.1) as $\alpha \to 0^+$. The stabilization process characterized as in (5.3) is called Tikhonov's regularization [16, 22, 23].

6. Numerical Examples

We will examine a numerical example, where we follow the procedure proposed in this paper to measure an impulsive movement of the sea bottom. For that, we first start with the following specification for the underwater displacement $F_0(x)$ in (2.5):

$$F_0(x) = 0.1e^{-c(x+4)^2} + 0.2e^{-cx^2} + 0.1e^{-c(x-4)^2} \quad (c > 0). \tag{6.1}$$

Note that the Fourier transform [30] of (6.1) is known as follows:

$$\widetilde{F}_0(k) = \mathbb{F}\{F_0(x)\} = 0.2\sqrt{\frac{\pi}{c}} e^{-k^2/4c} + 0.2\sqrt{\frac{\pi}{c}} \cos(4k). \tag{6.2}$$

We normalize the water depth h and the constant c as the unit. The water waves that result from this movement are briefly sketched in Figure 1. Graphical illustrations of $F_0(x)$ and its Fourier transform are depicted in Figures 2 and 3. In this paper, for numerical calculation, the interval for the physical variable x is taken as $-50 < x < 50$, and the interval for the frequency k as $-12 < k < 12$.

The impulsive movement of the sea bottom equation (6.1) leads to the generation of a wave system, the spatial distribution of which is

$$\eta_T(x, T) = \int_{-\infty}^{\infty} \frac{\cos\left\{T\sqrt{gk \tanh kh}\right\}}{2\pi \cosh kh} e^{ikx} \widetilde{F}_0(k) dk \tag{6.3}$$

from (3.2) at an elapsed (fixed) time T.

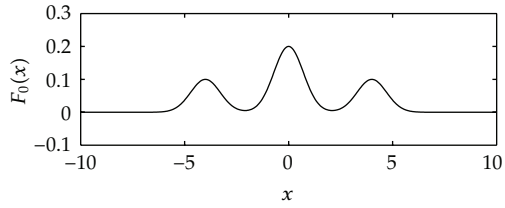

Figure 2: Graphical illustration of the impulsive movement $F_0(x)$ of the sea bottom in (6.1).

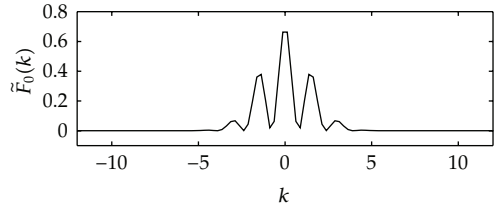

Figure 3: Fourier transform of $F_0(x)$ in (6.2).

6.1. Noise Level

Our aim is to inversely recover $F_0(x)$ in (6.1) by using the data η_T in (6.3). However, in practice, the measured (or calculated) data are always deteriorated somewhat due to noise. Thus, we assume that we know measured data, denoted by $\eta_{T,\delta}$. Thereby, we define a noise level $\delta > 0$, which satisfies the following norm inequality:

$$\left\| \frac{\eta_{T,\delta} - \eta_T}{\eta_T} \right\|_2 \leq \delta. \tag{6.4}$$

That is, the noise level is a quantity measuring an error intensity concerning the data $\eta_{T,\delta}$. Here, the notation $\|\cdot\|_2$ refers to the L_2 norm [23]. We have, in this study, the data $\eta_{T,\delta}$ randomly generated but with the two different noise levels δ of 10^{-4} and 10^{-6}, respectively. The noise is assumed to have the normal distribution with zero mean.

The numerical values for (6.3) are plotted in Figure 4(a) (noise-free condition), which shows the spatial wave distribution when $T = 10$. The results in Figures 4(b) and 4(c) correspond to the noise levels 10^{-4} and 10^{-6}.

6.2. Optimal Regularization Parameter

To achieve an accurate solution during the regularization, it is important to decide optimal regularization parameter in the Tikhonov regularization [16, 22, 23]. Based on the L-curve criterion [31], we depict the curves of log-log plot as shown in Figures 5 and 8:

$$\left(\log \left\| \mathfrak{L}_c q_\alpha - \eta_{T,\delta} \right\|_2,\ \log \left\| q_\alpha \right\|_2\right), \tag{6.5}$$

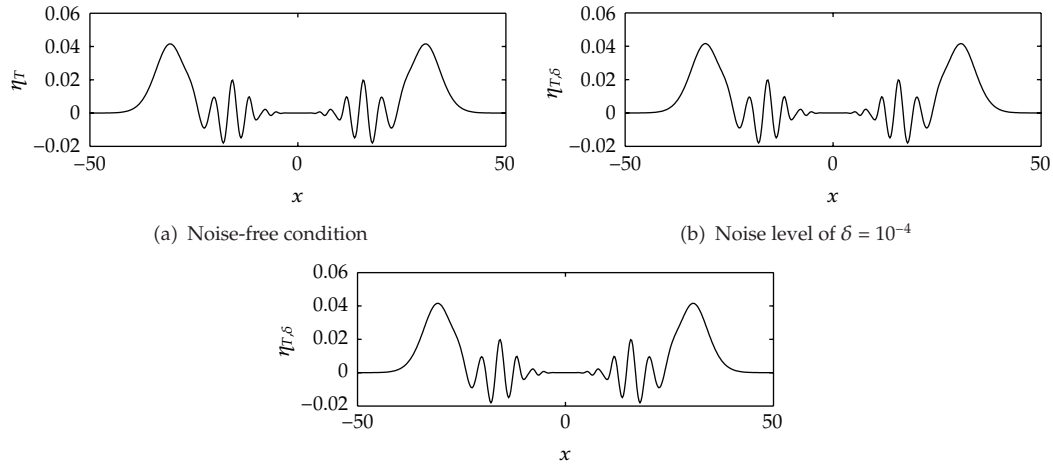

(a) Noise-free condition

(b) Noise level of $\delta = 10^{-4}$

(c) Noise level of $\delta = 10^{-6}$

Figure 4: The spatial distribution of the generated waves when $T = 10$ for a unit water depth at $-50 < x < 50$.

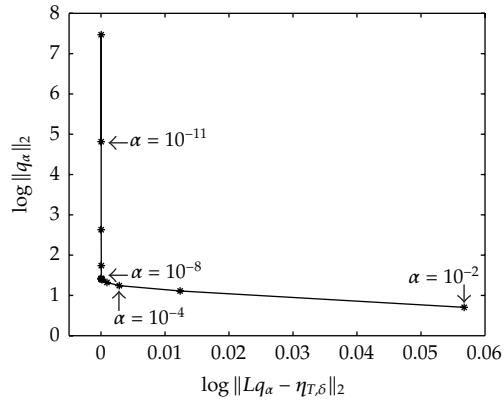

Figure 5: Illustration of the L-curve (noise level 10^{-4}). Note: the optimal regularization parameter ($\alpha = 10^{-8}$) occurs at the corner of the L-curve.

where q_α denotes the regularized solution, calculated by (5.3), depending on the regularization parameter α. Here, we discretize (5.3) directly; the Simpson's numerical integration rule is applied to the direct discretization. The number of intervals used for the Simpson's rule is chosen as 400. We obtain the optimal regularization parameter of $\alpha = 10^{-8}$ when the noise level is 10^{-4}. This is because the optimal regularization parameter corresponds to the corner of the L-curve in Figure 5 [31]. A brief explanation for this reason is as follows. When the regularization parameter α decreases, the size of error, $\|\mathfrak{L}_c q_\alpha - \eta_{T,\delta}\|_2$, reduces, because q_α approaches the true solution. However, subsequently q_α potentially deviates far away; that is, the function norm, $\|q_\alpha\|_2$, begins to increase, when $1/\alpha$ exceeds a certain threshold. This means that there exists an appropriate regularization parameter α such that the q_α is an optimal solution for the present problem. This optimal solution is shown to correspond to the corner of the L-curve by Hansen [31].

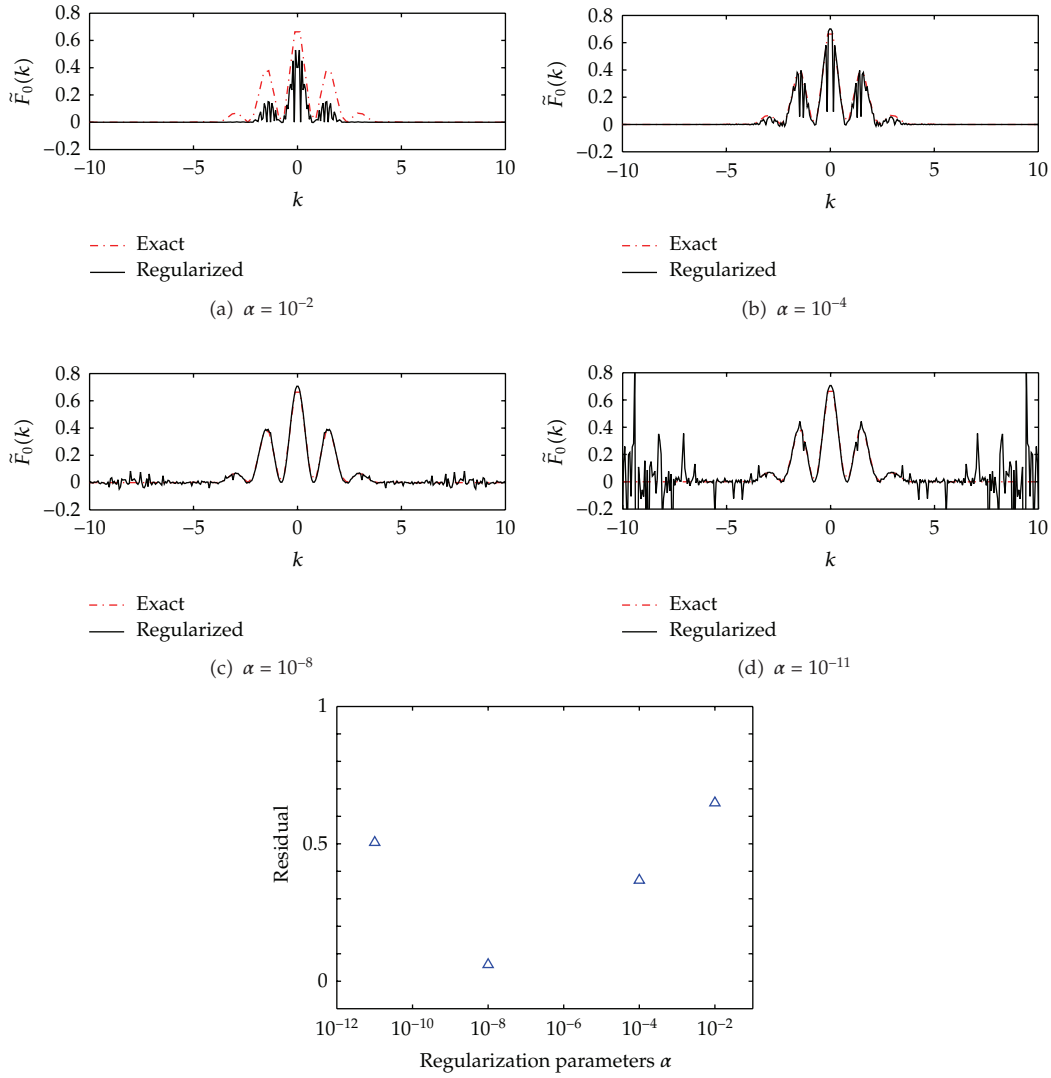

Figure 6: Comparison of the regularized wave spectrum with the exact one for four cases of regularization parameters α ((a)–(d): noise level 10^{-4}). Legend: the dotted and solid lines stand for the exact wave spectrum $\tilde{F}_0(k)$ in (6.2) and the (Tikhonov) regularized solution q_α in (5.3), respectively.

In a similar way, we can obtain the optimal regularization parameter $\alpha = 10^{-9}$ corresponding to the noise level 10^{-6}, as depicted in Figure 8.

6.3. Determining the Wave Spectrum

The graphs shown in Figures 6(a)–6(d), concerning the noise level 10^{-4}, compare the exact wave spectrum in (6.2) with the regularized wave spectrum q_α in (5.3). In addition,

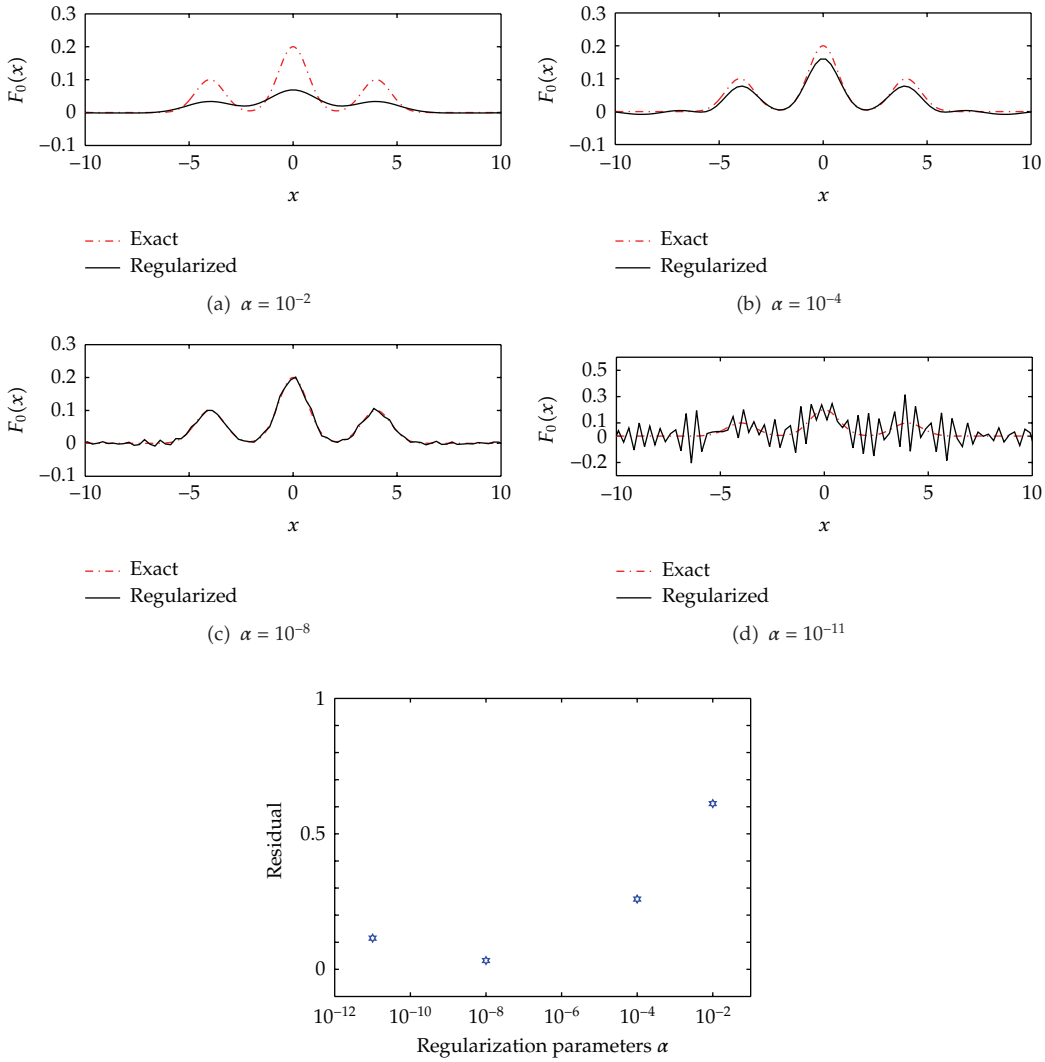

(e) Residual (the L_2 norm of difference between the exact and regularized displacement divided by the L_2 norm of the exact)

Figure 7: Comparison of the recovered sudden displacement of the sea bottom with the exact displacement for four cases of regularization parameters α ((a)–(d): noise level 10^{-4}). Legend: the dotted and solid lines stand for the exact $F_0(x)$ in (6.1) and the recovered sudden displacement of the sea bottom, respectively. The lines show good agreement with each other when the regularization parameter $\alpha = 10^{-8}$.

Figure 6(e) shows a residual, which is the L_2 norm of difference between the exact and regularized spectra divided by the L_2 norm of the exact. In fact, we did calculate many of various regularized wave spectra q_α with various values for α. Among them, only four selected regularization parameters $\alpha(= 10^{-2}, 10^{-4}, 10^{-8}$, and $10^{-11})$ are depicted in Figures 6(a)–6(d). This immediately shows that the best approximation for the wave spectrum is found, when the regularization parameter α equals 10^{-8}; as mentioned above, this value of α is an optimal regularization parameter corresponding to the corner of the L-curve.

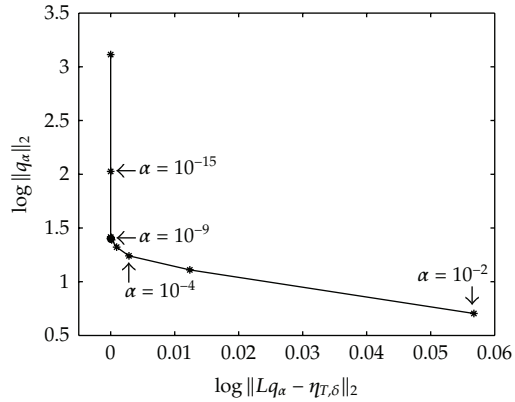

Figure 8: Illustration of the L-curve (noise level 10^{-6}). Note: The optimal regularization parameter ($\alpha = 10^{-9}$) occurs at the corner of the L-curve.

Similarly, when the noise level is equal to 10^{-6}, we did carry out a lot of calculations of regularized wave spectra q_α for various regularization parameters α. We also select only four $\alpha(= 10^{-2}, 10^{-4}, 10^{-9}$, and $10^{-15})$ among them, as shown in Figures 9(a)–9(d), and the residual is seen in Figure 9(e). Here, the exact wave spectra are compared with the regularized ones q_α. It is clear from Figure 9 that the best approximation to the exact one occurs when $\alpha = 10^{-9}$, which was anticipated from the L-curve in Figure 8.

6.4. Recovering $F_0(x)$

Following (3.5), we can recover the sudden movement of the sea bottom $F_0(x)$, which are depicted in Figures 7(a)–7(d) and in Figures 10(a)–10(d). Here, the residual is also calculated and depicted in Figures 7(e) and 10(e), respectively. There are fairly good agreements between the exact and recovered results. The most accurate results are found when the regularization parameters are optimal.

7. Discussions

We proposed a new method to find sudden movements of the sea bottom using just a local snapshot data of wave configurations, $-\ell < x < l$. However, it is interesting to observe also how the method proposed is suitable to retrieve whole wave configurations, that is, we can identify $\eta_T = \eta(x,T)$, $-\infty < x < \infty$, just using a local data $\eta(x,T)$, $-\ell < x < l$. This is realized by simply estimating the integration

$$\eta_T = \int_{-\kappa}^{\kappa} K(x,T,k) q_\alpha(k) dk, \tag{7.1}$$

where $q_\alpha(k)$ is a Tikhonov's regularized solution in (5.3).

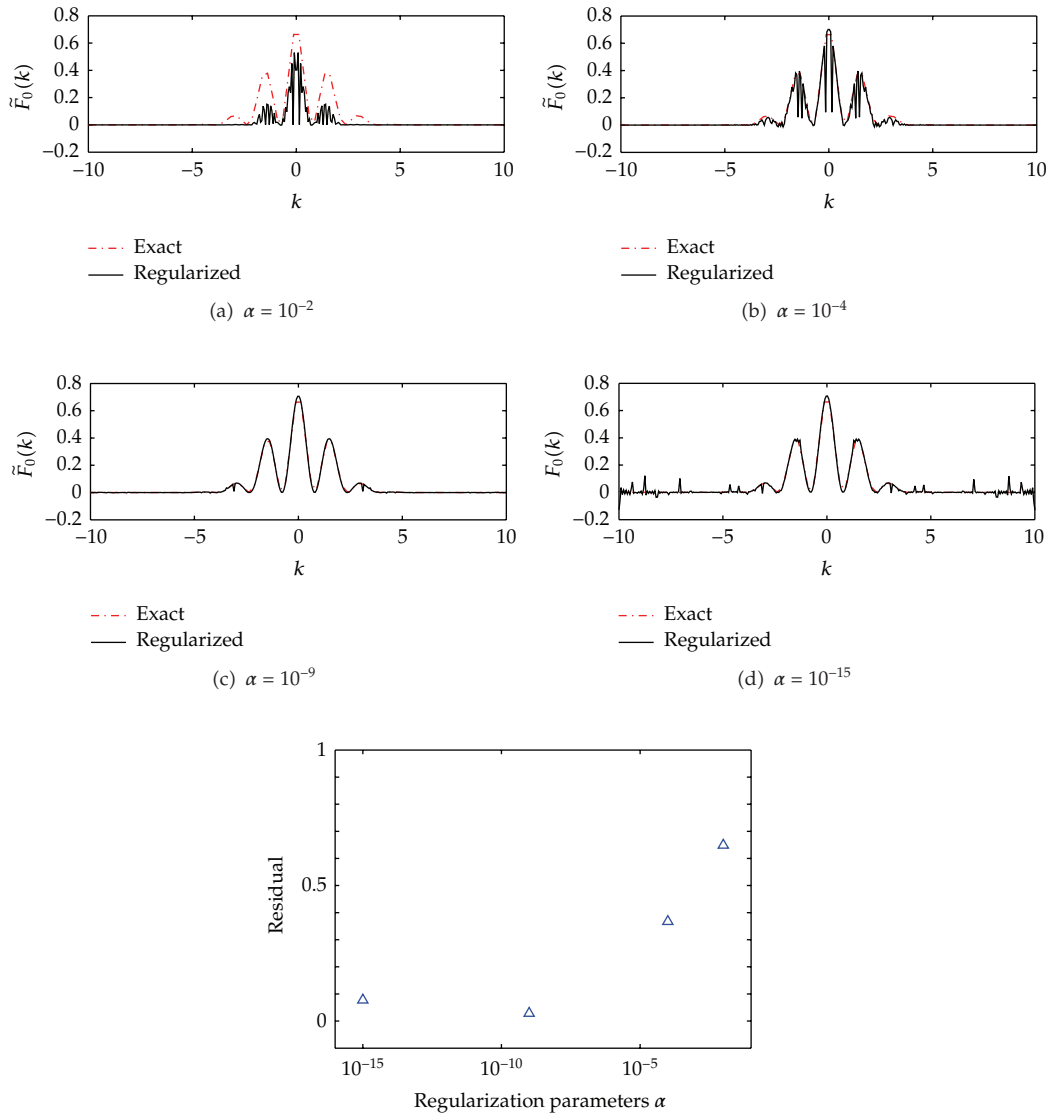

(e) Residual (the L_2 norm of difference between the exact and regularized spectra divided by the L_2 norm of the exact)

Figure 9: Comparison of the regularized wave spectrum with the exact wave spectrum for four cases of regularization parameters α ((a)–(d): noise level 10^{-6}). Legend: the dotted and solid lines stand for the exact wave spectrum $\widetilde{F}_0(k)$ in (6.2) and the (Tikhonov) regularized solution q_α in (5.3), respectively.

In the present inverse study, we assumed that the sea bottom movement is instantaneous. In fact, this may be a usual assumption in these kinds of wave generation problems, especially studying tsunamigenic earthquakes. However, sometimes the sea bottom movement can be relatively slow, for example in case of a tsunami earthquake [32]. In this case, the sea bottom movement is not considered to be instantaneous, which means that the inverse method proposed in this study does not work.

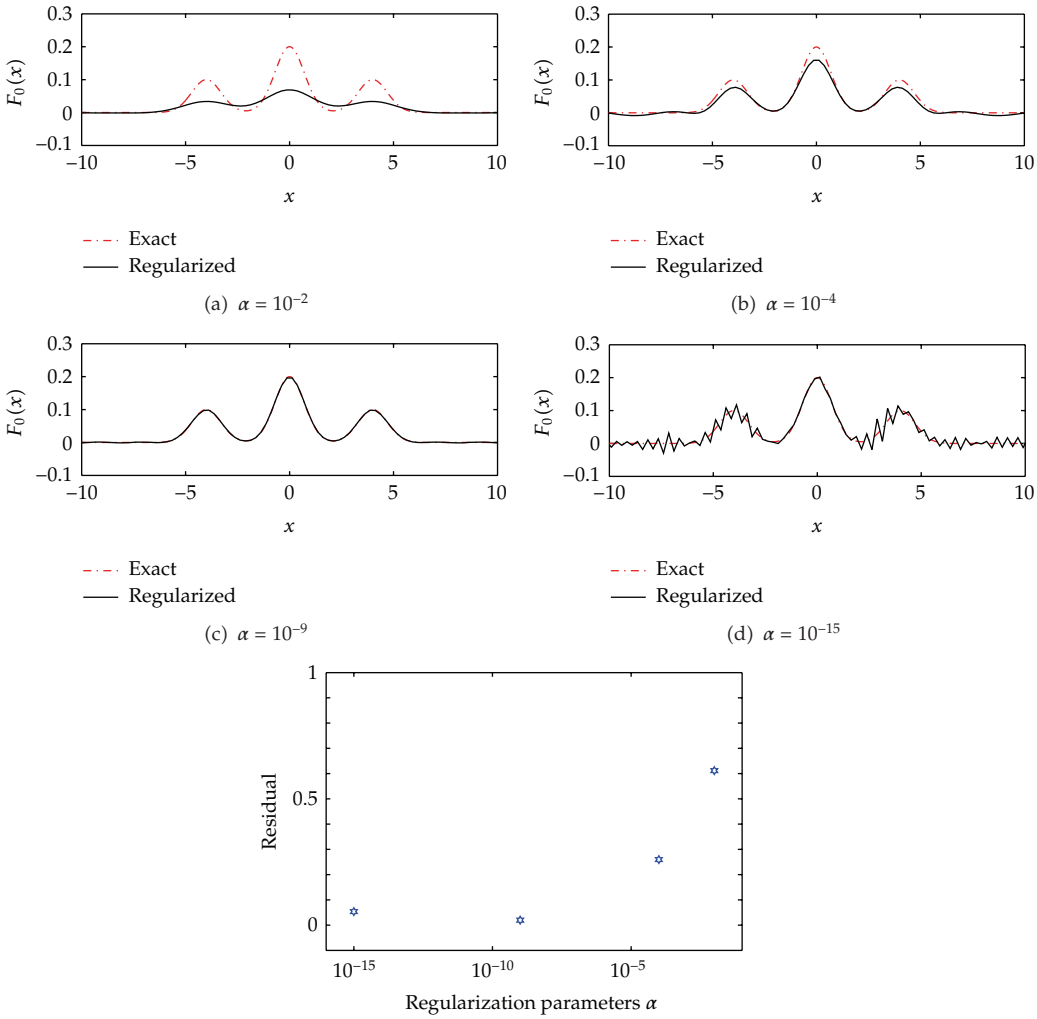

(e) Residual (the L_2 norm of difference between the exact and regularized displacement divided by the L_2 norm of the exact)

Figure 10: Comparison of the recovered, sudden displacement of the sea bottom with the exact displacement for four cases of regularization parameters α ((a)–(d): noise level 10^{-6}). Legend: the dotted and solid lines stand for the exact $F_0(x)$ in (6.1) and the recovered sudden displacement of the sea bottom, respectively. The lines show good agreement with each other when the regularization parameter $\alpha = 10^{-9}$.

8. Conclusion

Sudden underwater movements of the sea bottom result in the free-surface flow of ocean waves. The problem of finding the resulting wave flow is well studied, and is known as the forward problem. We examine whether an inverse problem can be defined as an alternative approach. We explore whether it is possible to indirectly measure sudden underwater movements using a local snapshot data of the resulting wave motion. We propose an indirect measurement procedure that successfully confirms the viability of the inverse problem approach. A numerical example is presented that verifies the proposed procedure and

confirms its workability. As application, it is interesting and important to know that if we have a local snapshot data of wave configurations by remote control airplane, we can recover a wider range of wave configuration, of course, including the local data, by using the method proposed in this study.

Acknowledgments

This work is partially supported by the principal R&D program of KORDI: "Performance Evaluation Technologies of Offshore Operability for Transport and Installation of Deep-sea Offshore Structures" granted by Korea Research Council of Public Science and Technology. In addition, the first author and the third author are partially supported by Basic Science Research Program through the National Research Foundation of Korea (NRF) funded by the Ministry of Education, Science and Technology (Grant no.: 2011-0010090). And they were also supported by Basic Science Research Program through the National Research Foundation of Korea (NRF) funded by the Ministry of Education, Science and Technology (Grant no.: K20902001780-10E0100-12510).

References

[1] C. C. Mei, *The Applied Dynamics of Ocean Surface Waves*, World Scientific, London, UK, 1989.
[2] J. J. Stoker, *Water Waves*, Wiley-Interscience, 1992.
[3] G. B. Whitham, *Linear and Nonlinear Waves*, Wiley-Interscience, 1999.
[4] J. T. Kirby and R. A. Dalrymple, "An approximate model for nonlinear dispersion in monochromatic wave propagation models," *Coastal Engineering*, vol. 9, no. 6, pp. 545–561, 1986.
[5] T. S. Jang, S. L. Han, and T. Kinoshita, "An inverse measurement of the sudden underwater movement of the sea-floor by using the time-history record of the water-wave elevation," *Wave Motion*, vol. 47, no. 3, pp. 146–155, 2010.
[6] D. A. Sotiropoulos and J. D. Achenbach, "Crack characterization by an inverse scattering method," *International Journal of Solids and Structures*, vol. 24, no. 2, pp. 165–175, 1988.
[7] J. D. Achenbach, K. Viswanathan, and A. Norris, "An inversion integral for crack-scattering data," *Wave Motion*, vol. 1, no. 4, pp. 299–316, 1979.
[8] M. Cheney and D. Isaacson, "Inverse problems for a perturbed dissipative half-space," *Inverse Problems*, vol. 11, no. 4, article 015, pp. 865–888, 1995.
[9] A. L. Mazzucato and L. V. Rachele, "On uniqueness in the inverse problem for transversely isotropic elastic media with a disjoint wave mode," *Wave Motion*, vol. 44, no. 7-8, pp. 605–625, 2007.
[10] J. Janno and J. Engelbrecht, "Waves in microstructured solids: inverse problems," *Wave Motion*, vol. 43, no. 1, pp. 1–11, 2005.
[11] N. Dominguez, V. Gibiat, and Y. Esquerre, "Time domain topological gradient and time reversal analogy: an inverse method for ultrasonic target detection," *Wave Motion*, vol. 42, no. 1, pp. 31–52, 2005.
[12] H. Hellsten, V. Maz'ya, and B. Vainberg, "The spectrum of water waves produced by moving point sources, and a related inverse problem," *Wave Motion*, vol. 38, no. 4, pp. 345–354, 2003.
[13] T. S. Jang, H. Baek, S. L. Han, and T. Kinoshita, "Indirect measurement of the impulsive load to a nonlinear system from dynamic responses: inverse problem formulation," *Mechanical Systems and Signal Processing*, vol. 24, pp. 1665–1681, 2010.
[14] T. S. Jang, H. S. Baek, and J. K. Paik, "A new method for the non-linear deflection analysis of an infinite beam resting on a non-linear elastic foundation," *International Journal of Non-Linear Mechanics*, vol. 46, no. 1, pp. 339–346, 2011.
[15] T. S. Jang, "Non-parametric simultaneous identification of both the nonlinear damping and restoring characteristics of nonlinear systems whose dampings depend on velocity alone," *Mechanical Systems and Signal Processing*, vol. 25, no. 4, pp. 1159–1173, 2011.
[16] A. Kirsch, *An Introduction to the Mathematical Theory of Inverse Problems*, Springer, 1996.

[17] L. Patrick and L.-F. L. Philip, "A numerical study of submarine–landslide–generated waves and run–up," *Proceedings of the Royal Society of London A*, vol. 458, no. 2028, pp. 2885–2910, 2002.

[18] K. Satake, "Inversion of tsunami waveforms for the estimation of a fault heterogeneity: method and numerical experiments," *Journal of the Physics of the Earth*, vol. 35, pp. 241–254, 1987.

[19] J. M. Johnson, K. Satake, S. R. Holdahl, and J. Sauber, "The 1964 prince William sound earthquake: joint inversion of tsunami and geodetic data," *Journal of Geophysical Research B*, vol. 101, no. 1, pp. 523–532, 1996.

[20] Y. Wei, K. F. Cheung, G. D. Curtis, and C. S. McCreery, "Inverse algorithm for tsunami forecasts," *Journal of Waterway, Port, Coastal and Ocean Engineering*, vol. 129, no. 2, pp. 60–69, 2003.

[21] B. L. Mehaute and S. Wang, *Water Waves Generated by Underwater Explosion*, World Scientific, London, UK, 1996.

[22] C. W. Groetsch, *Inverse Problems in the Mathematical Sciences*, Vieweg, 1993.

[23] T. S. Jang, H. S. Choi, and S. L. Han, "A new method for detecting non-linear damping and restoring forces in non-linear oscillation systems from transient data," *International Journal of Non-Linear Mechanics*, vol. 44, no. 7, pp. 801–808, 2009.

[24] T. S. Jang and T. Kinoshita, "An ill-posed inverse problem of a wing with locally given velocity data and its analysis," *Journal of Marine Science and Technology*, vol. 5, no. 1, pp. 16–20, 2000.

[25] T. S. Jang, H. S. Choi, and T. Kinoshita, "Numerical experiments on an ill-posed inverse problem for a given velocity around a hydrofoil by iterative and noniterative regularizations," *Journal of Marine Science and Technology*, vol. 5, no. 3, pp. 107–111, 2000.

[26] T. S. Jang, H. S. Choi, and T. Kinoshita, "Solution of an unstable inverse problem: wave source evaluation from observation of velocity distribution," *Journal of Marine Science and Technology*, vol. 5, no. 4, pp. 181–188, 2001.

[27] T. S. Jang, S. H. Kwon, and B. J. Kim, "Solution of an unstable axisymmetric Cauchy-Poisson problem of dispersive water waves for a spectrum with compact support," *Ocean Engineering*, vol. 34, no. 5-6, pp. 676–684, 2007.

[28] T. S. Jang and S. L. Han, "Application of Tikhonov's regularization to unstable water waves of the two-dimensional fluid flow: spectrum with compact support," *Ships and Offshore Structures*, vol. 3, no. 1, pp. 41–47, 2008.

[29] T. S. Jang, H. G. Sung, S. L. Han, and S. H. Kwon, "Inverse determination of the loading source of the infinite beam on elastic foundation," *Journal of Mechanical Science and Technology*, vol. 22, no. 12, pp. 2350–2356, 2008.

[30] M. R. Spiegel, *Mathematical Handbook*, McGraw-Hill, 1968.

[31] P. C. Hansen, "Analysis of discrete ill-posed problems by means of the L-curve," *SIAM Review*, vol. 34, pp. 561–580, 1992.

[32] H. Kanamori, "Mechanism of tsunami earthquakes," *Physics of the Earth and Planetary Interiors*, vol. 6, no. 5, pp. 346–359, 1972.